Heliyon 8 (2022) e09068

Contents lists available at ScienceDirect

Heliyon

journal homepage: www.cell.com/heliyon

Research article

Integrated multi-omics analysis reveals miR-20a as a regulator for metabolic colorectal cancer

Kai Song [a,c,1], Chao Liu [b,1], Jiashuai Zhang [a], Yang Yao [b], Huiting Xiao [a], Rongqiang Yuan [a], Keru Li [a], Jia Yang [a], Wenyuan Zhao [a,*], Yanqiao Zhang [b,**]

[a] College of Bioinformatics Science and Technology, Harbin Medical University, Harbin, 150086, China
[b] Department of Gastrointestinal Medical Oncology, Harbin Medical University Cancer Hospital, Harbin, 150086, China
[c] Zhuhai Interventional Medical Center, Zhuhai Precision Medical Center, Zhuhai People's Hospital, Zhuhai Hospital Affiliated with Jinan University, Jinan University, Zhuhai, Guangdong, 519000, China

ARTICLE INFO

Keywords:
miRNA
Consensus molecular subtype
Fatty acid metabolism
Wnt signaling pathway
Metabolic colorectal cancer

ABSTRACT

Single-driver molecular events specific to the metabolic colorectal cancer (CRC) have not been clearly elucidated. Herein, we identified 12 functional miRNAs linked to activated metabolism by integrating multi-omics features in metabolic CRC. These miRNAs exhibited significantly enriched CRC driver miRNAs, significant impacts on CRC cell growth and significantly correlated metabolites. Importantly, miR-20a is minimally expressed in normal colorectal tissues but highly expressed in metabolic CRC, suggesting the potential therapeutic target. Bioinformatics analyses further revealed miR-20a as the most powerful determinant that regulates a cascade of dysregulated events, including Wnt signaling pathway, core enzymes involved in FA metabolism program and triacylglycerol abundances. In vitro assays demonstrated that elevated miR-20a up-regulated FA synthesis enzymes via Wnt/β-catenin signaling, and finally promoted proliferative and migration of metabolic CRC cells. Overall, our study revealed that miR-20a promoted progression of metabolic CRC by regulating FA metabolism and served as a potential target for preventing tumor metastasis.

1. Introduction

Colorectal carcinoma (CRC) ranks the second leading cause of cancer-related deaths worldwide, with high heterogeneity at the molecular level (Sottoriva et al., 2015). The consensus molecular subtypes (CMSs) of CRC were proposed: CMS1 (microsatellite instability immune, 14%); CMS2 (canonical, 37%); CMS3 (metabolic, 13%); and CMS4 (mesenchymal, 23%) (Guinney et al., 2015). CMSs present with differences in molecular characteristics and clinical outcomes. Patients with canonical CMS2 have the best outcome, while mesenchymal CMS4 tumors have a poor outcome and CMS1 is associated with a poor patient survival after relapse. In contrast, CMS3 which is defined as metabolic CRC and characterized by prominent metabolic activation and disturbed fatty acid (FA) metabolism, had intermediate overall survival and has received less attention. FA metabolism maintains energy homeostasis (Kim and DeBerardinis, 2019), plays a major role in the growth and progression of cancers in cancer (Jones and Infante, 2015; Long et al., 2018), and is regarded as a new therapeutic strategy (Bruning et al., 2018). The regulation of FA metabolism and clinical value within CMS3 tumors remains unknown.

A microRNA (miRNA) is a small non-coding RNA molecule that functions as post-transcriptional gene regulators (Bartel, 2018). Individual microRNA can affect many genes simultaneously, underscoring their influence on the expression of complete networks determining a specific cancer subtype. miRNAs serve important roles in several physiological conditions, including cell differentiation, development, apoptosis, immune response, hematopoiesis, cell death and proliferation (Hammond, 2015; Kim et al., 2009). For example, miR-20a promote CRC proliferation and invasion (Xiao et al., 2020), and served as a predictor of poor prognosis in CRC (Moody et al., 2019). However, the role of miR-20a in metabolic CRC has not been analyzed. In recent years, researches have shown that miRNAs regulate FA metabolism in cancers (Chan et al., 2015). It has been demonstrated that miR-185 and miR-342 control lipogenesis in prostate cancer cells by down-regulating fatty acid

* Corresponding author.
** Corresponding author.
E-mail addresses: zhaowenyuan@ems.hrbmu.edu.cn (W. Zhao), yanqiaozhang@ems.hrbmu.edu.cn (Y. Zhang).
[1] These authors have contributed equally to this work: Kai Song, Chao Liu.

https://doi.org/10.1016/j.heliyon.2022.e09068
Received 8 November 2021; Received in revised form 21 December 2021; Accepted 3 March 2022

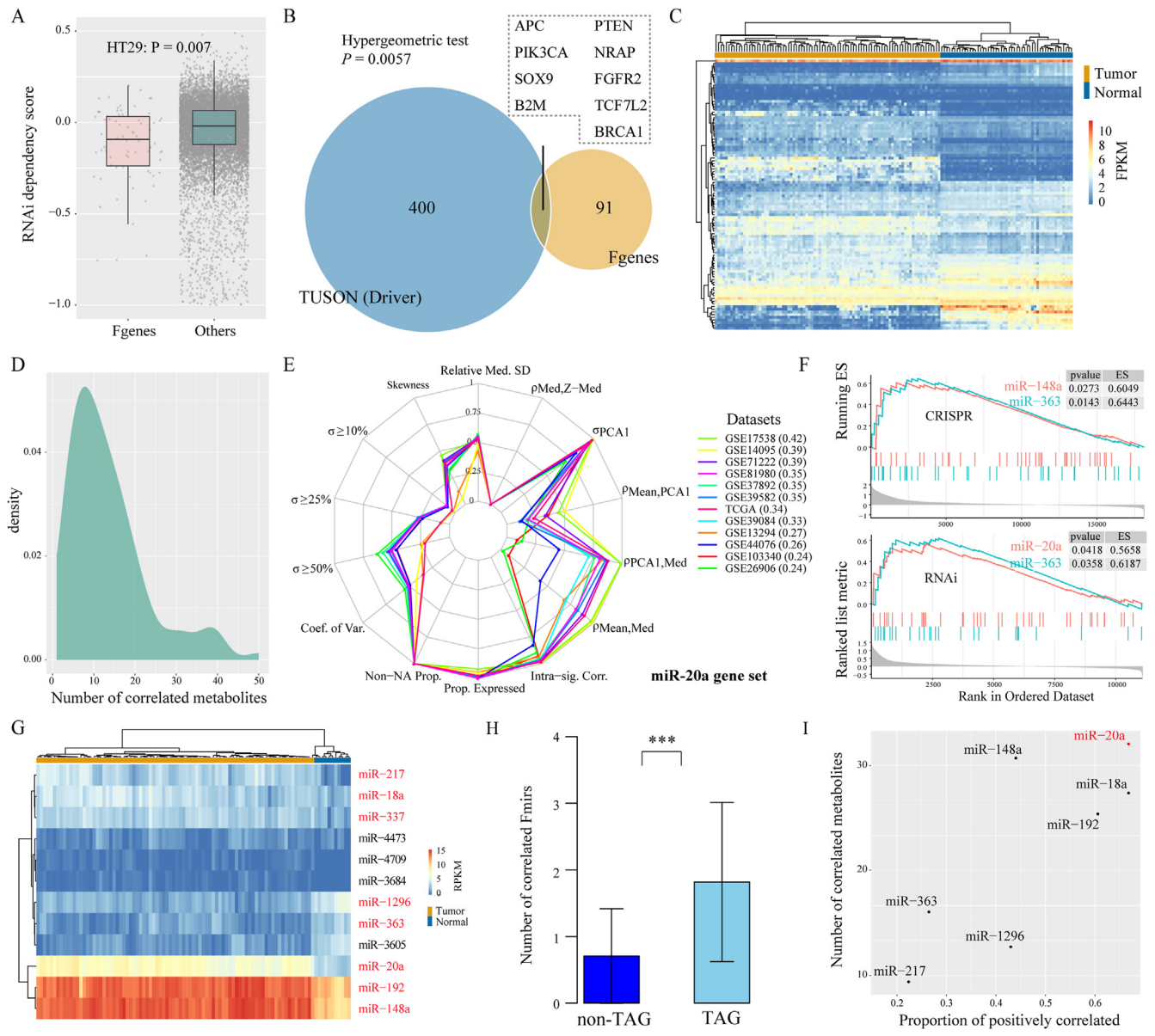

Figure 1. Identification of functional miRNAs. (A) Comparison of Mgenes and other genes in RNAi dependency scores of HT29. (B) Venn diagram illustrates that Mgenes were enriched with tumor driver genes identified by TUSON. (C) Heatmaps show that the expression of Mgenes can separate the metabolic CRC samples from normal samples. (D) A density plot shows the distribution of correlated metabolites for Mgenes. (E) Evaluating the basic statistical properties of gene set signatures underlying their applicability across datasets using sigQC. (F) GSEA confirmed Fmirs were significantly overrepresented at the top of gene list in ascending order in the RNAi and CRISPR screened HT29 cell lines. (G) Heatmaps show that the expression of Fmirs can separate the metabolic CRC samples from normal samples. (H) Comparison of correlated Fmirs between TAG and non-TAG. (I) Number of significantly correlated metabolites vs. the proportion of positively correlated metabolites for Fmirs.

synthase (Li et al., 2013). miR-20a was also a potential regulator of lipid metabolism in nonalcoholic fatty liver disease (Zhang et al., 2021). However, many researchers seem to focus more on the regulation of miRNAs on FA metabolism in other diseases than CRC. The role of miRNAs in metabolic CRC remains mostly unexplored.

Multi-omics datasets represent distinct aspects of the central dogma of molecular biology, emphasizing the complementarity of underlying biology (Paczkowska et al., 2020). Previously, we proposed to prioritize functional gene regulators in CMSs by integrating genome, epigenome, transcriptome and interactome data, which play central roles in the corresponding subtypes (Song et al., 2021). Herein, we proposed to prioritize functional miRNAs (Fmirs) linked to activated metabolism in metabolic CRC by identifying functional genes involving in metabolism (Mgenes) and constructing miRNA-Mgene interaction network. We found that these miRNAs were enriched with driver miRNAs of CRC and mediated FA metabolism. Functional assays showed miR-20a led to an increase in FA synthesis enzymes, and regulated proliferation and migration of metabolic CRC via Wnt signaling pathway.

2. Materials and methods

2.1. Data source

We downloaded publicly available CRC gene expression datasets from Gene Expression Omnibus (GEO; https://www.ncbi.nlm.nih.gov/gds/) and The Cancer Genome Atlas (TCGA; https://portal.gdc.cancer.gov/) (Table S1). We collected a set of 3,360 CRC tissue samples from 21 datasets measured by eight platforms and another set of 618 adjacent

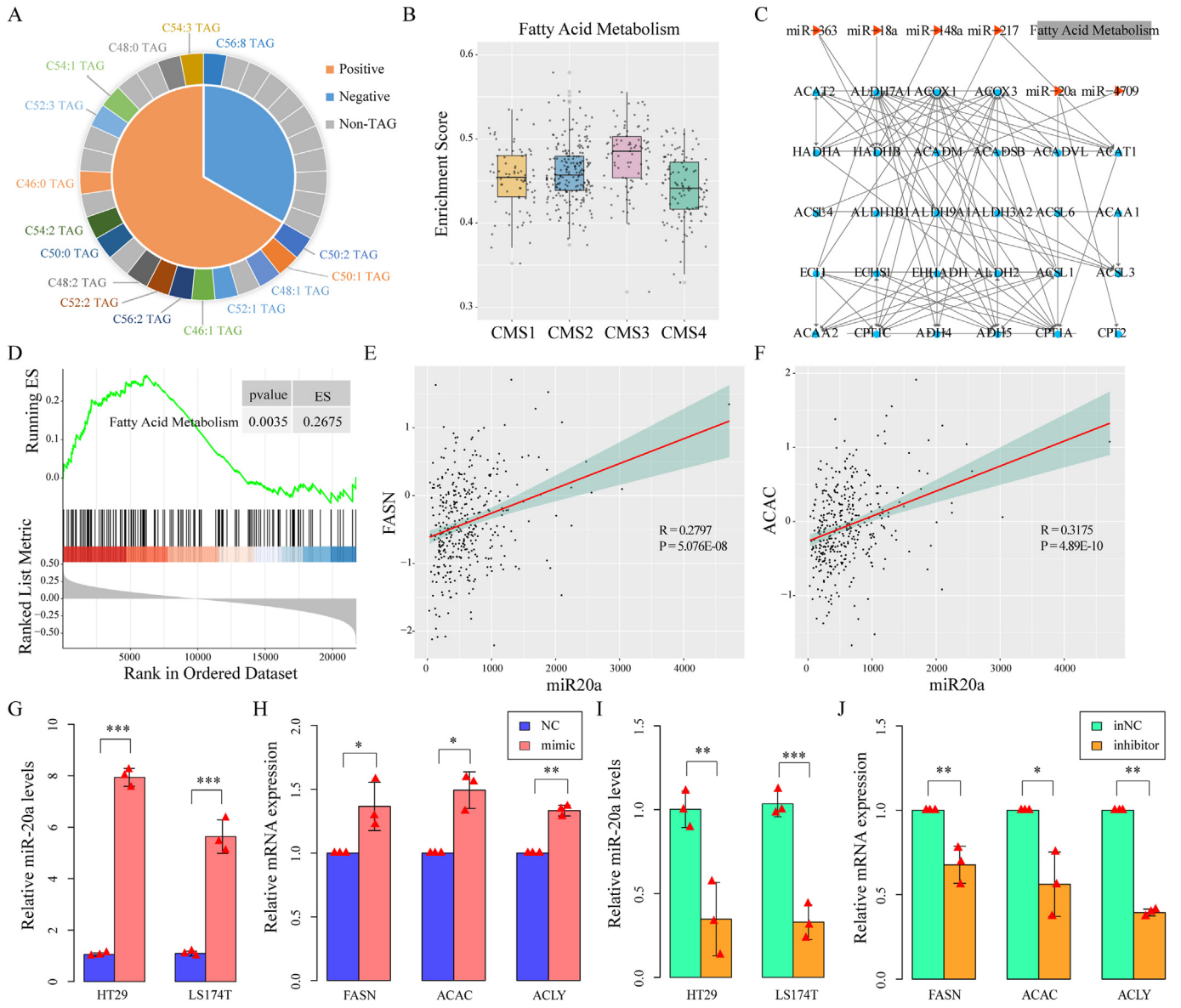

Figure 2. miR-20a regulated FA metabolism. (A) The correlated metabolites of miR-20a. (B) FA metabolism pathway showed significantly higher ES in metabolic CRC than other subtypes. (C) Fmirs participated in FA metabolism subpathway. (D) GSEA showed hallmark gene set of FA metabolism was upregulated in miR-20a high expression group. (E–F) Correlation of miR-20a expression with protein expression of FA metabolism enzymes. (G) RT-qPCR analysis of the expression of miR-20a in HT29 and LS174T cells transfected with miR-20a mimics and their NC groups. (H) RT-qPCR analysis of the expression of FA synthesis related genes in HT29 after transfected with miR-20a mimic. (I) RT-qPCR analysis of the expression of miR-20a in HT29 and LS174T cells transfected with miR-20a inhibitor groups and their NC groups. (J) RT-qPCR analysis of the expression of FA synthesis related genes in HT29 after transfected with miR-20a inhibitor. Statistical analysis was conducted using one-way ANOVA. (*$P < 0.05$; **$P < 0.01$; ***$P < 0.001$).

normal tissue samples from 23 datasets measured by six platforms. Only 12,401 genes that are shared in all these datasets were used. Especially for CRC samples, we only used the datasets containing more than 50 samples to avoid the influence of small sample bias. Data were pre-processed as previously described (Song et al., 2020).

We also downloaded 619 miRNA samples, 536 mutation samples analyzed by MuTect 2 algorithm (.maf files), 617 copy number alteration (CNA) samples and 295 DNA methylation samples from the TCGA project (TCGA-COAD and TCGA-READ). Protein expression data were downloaded from the Cancer Proteome Atlas (TCPA).

2.2. Classification of colorectal cancer tissue samples

The random forest classifyCMS function in the R package CMSclassifier (https://github.com/Sage-Bionetworks/CMSclassifier) was used to assign CMSs to CRC samples based on the gene expression profile of each tissue dataset (Guinney et al., 2015). Microarray data for all datasets were obtained in the form of normalized expression values on the log2 scale. For RNAseq data, we used log2 transformed FPKM matrix after adding 1 to avoid undefined values.

2.3. Colorectal cancer cell lines

The gene expression data, miRNA expression and metabolite abundances of 57 large intestine cell lines were download from the Cancer Cell Line Encyclopedia (CCLE) database (https://portals.broadinstitute.org/ccle). The CMScaller algorithm was used to assign CMSs to CRC cell lines (https://github.com/Lothelab/CMScaller). CMS cell lines were also supplemented with the reported results (Eide et al., 2017).

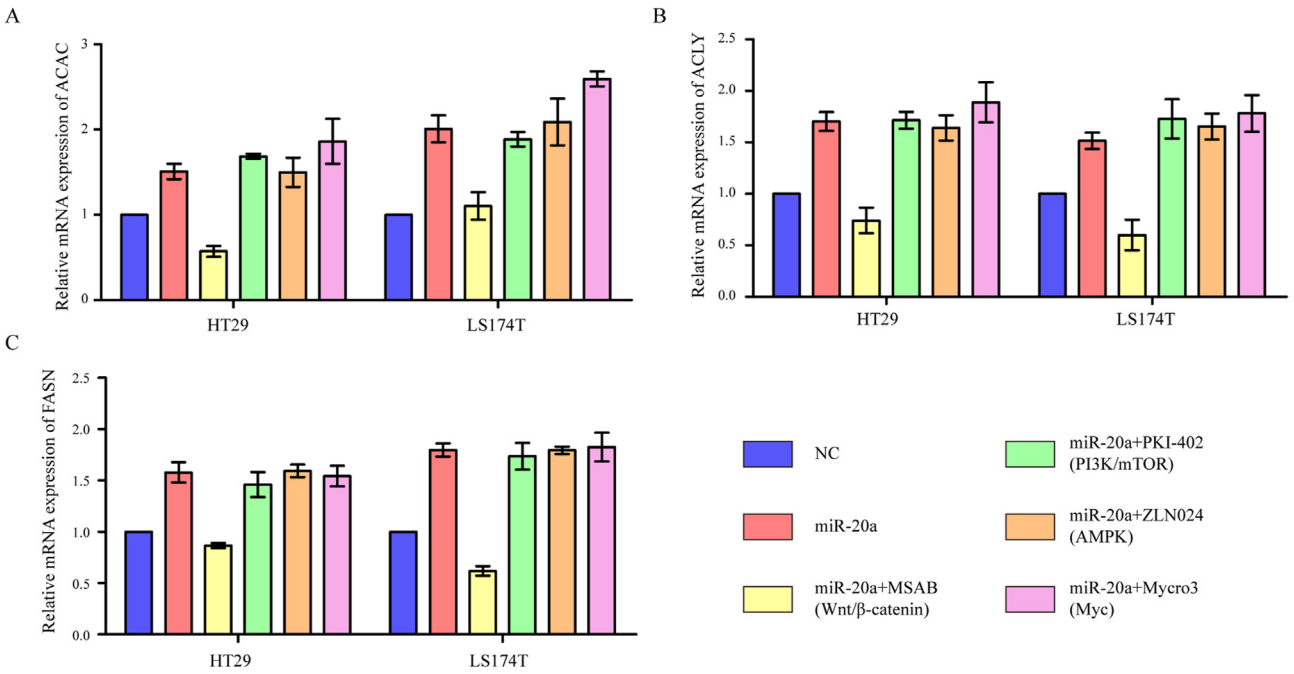

Figure 3. Screening the pathway of miR-20a promoting FA synthesis from PI3K/AKT/mTOR, Wnt, Myc and AMPK pathway by inhibitors/activators. (A) ACAC. (B) ACLY. (C) FASN.

2.4. Manually curation of gene interaction

Protein–protein interaction network (PPIN) data were downloaded from STRING v11.0 (https://string-db.org/) (Szklarczyk et al., 2019). We used interactions with the organism of "Homo sapiens" and score more than 0.9 with high confidence. TF–gene interactions assayed by chromatin immunoprecipitation followed by sequencing (ChIP-seq) were also downloaded from the ChIPBase v2.0 database (http://rna.sysu.edu.cn/chipbase/) (Zhou et al., 2017).

PPI and TF–gene interactions in the context of metabolic CRC were filtered based on their expression correlation measured by the Pearson correlation analysis. We only retained the significantly co-expressed interactions with the threshold of adjusted $P < 0.05$ and $|\rho|>0.3$. "ρ" represents the Pearson correlation coefficient.

2.5. miRNA-mediated gene regulation

miRNA–gene interactions were all experimentally validated and collected from public databases, including TarBase (Karagkouni et al., 2018), miRTarBase (Huang et al., 2020), and miRecords (Xiao et al., 2009). miRNA–gene regulations in the context of metabolic CRC were filtered based on their expression correlation measured by the Pearson correlation analysis with the threshold of $P < 0.05$ and $|\rho|>0.3$.

We note that these target genes of miRNAs were derived from TCGA data. To avoid biased results, we took the target genes as a gene signature for each miRNA and performed an evaluation step (sigQC) to ensure that the signature used has suitable properties across different datasets. Here, we present radar plots summarizing the gene signature quality control metrics implemented by the R package sigQC (Dhawan et al., 2019).

2.6. Identification of functional miRNAs

We identified Fmirs by firstly identifying Mgenes. Based on the individual-level differentially expressed genes calculated by RankComp algorithm (Wang et al., 2015). We identified genes with significantly up- or down-regulated patterns and defined them as metabolism-related genes in metabolic CRC. Then, we proposed a computational method to prioritize metabolism-related genes and identify Mgenes by integrating multi-omics features (Song et al., 2021). Briefly, for each metabolism-related gene in metabolic CRC, we calculated the scores of seven features that characterized the genomic and transcriptomic activity, regulation by co-expressed TFs, and central roles in PPIN of gene regulators. The aggregated score for each gene was further calculated by integrating the seven separate ranks in metabolic CRC, using the robust rank aggregation method in R package RobustRankAggreg (Kolde et al., 2012). Then, we utilized the most effective feature and identified top-ranked 100 genes as the Mgenes.

For miRNA, we directly analyzed the 1,881 miRNAs measured by the TCGA-COAD and TCGA-READ project. We identified Fmirs using a backward derivation approach. Firstly, we identified significantly co-expressed miRNA and genes for metabolic CRC among the collected miRNA-gene interactions. Then, miRNAs whose target genes were significantly intersected with Mgenes were defined as Fmirs. The hypergeometric test was used to calculate the significance as follows:

$$\Pr(i) = 1 - \sum_{x=0}^{F_i-1} \frac{\binom{T_i}{x}\binom{N-T_i}{F-x}}{\binom{N}{F}} \quad (1)$$

where N is the number of target genes that overlap with all detected genes in the expression profiles, F is the number of target genes that overlap with Mgenes, T_i is the number of target genes of miRNA i, and F_i is the number of target genes for miRNA i that overlap with Mgenes.

2.7. Manually curation of CRC driver miRNAs

A panel of oncogenic and tumor-suppressive miRNAs was collected from the public databases miRCancer (Xie et al., 2013) and OncomiRDB (Wang et al., 2014). Briefly, the microRNA–cancer association in miRCancer was extracted using the text mining algorithm against PubMed based on 75 rules. The entries of CRC-related miRNA regulations in OncomiRDB were manually curated from abstracts with direct experimental evidence. Finally, we retained miRNAs associated with CRC and collected 250 CRC-related miRNAs.

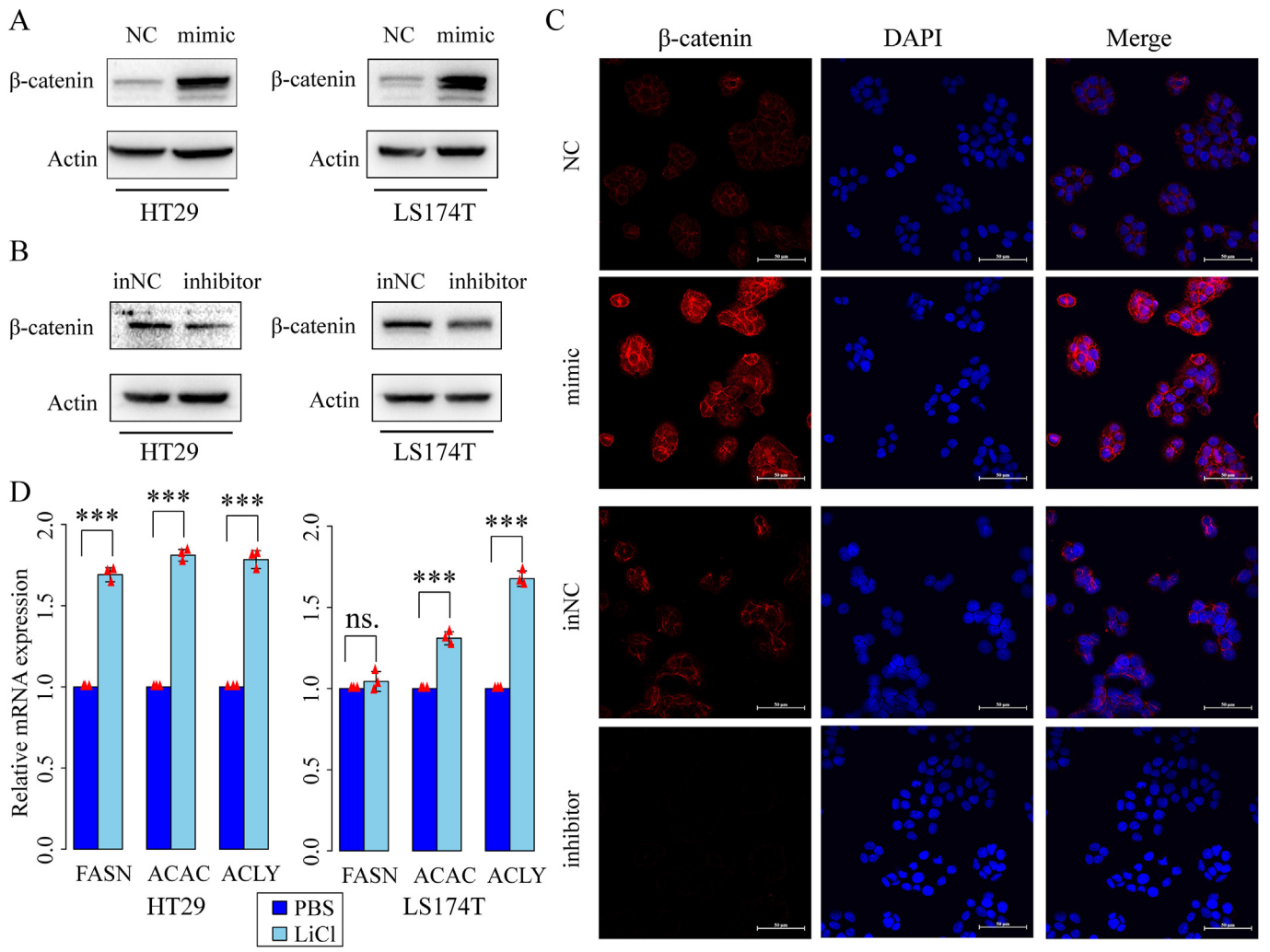

Figure 4. Correlation of miR-20a with Wnt signaling pathway. (A–B) Western blotting of β-catenin in HT29 and LS174T cells transfected with different miRNAs. (C) Representative photomicrographs of β-catenin immunofluorescence staining assay in HT29 cells. Bar = 50μm. (D) RT-qPCR analysis of the expression of FA synthesis related genes (FASN, ACAC and ACLY) in HT29 and LS174T after treated with LiCl (10 mmol/L) for 24h. (***P < 0.001; ns, not significant).

2.8. Subpathway analysis

The R package "Subpathway-GMir" was performed to identify the metabolism subpathways mediated by miRNAs(Feng et al., 2015). We mapped the Fmirs and significantly co-expressed target genes as nodes into the reconstructed metabolism pathway graphs obtained from the package. Then, we identified miRNA-mediated FA metabolism subpathways based on the "lenient distance" similarity method. It evaluated the significance of candidate subpathways using the hypergeometric method. The miRNA–target interactions for metabolic CRC were collected as described above.

2.9. Experimental model and subject details

2.9.1. Cell culture and transfection

Human colon epithelial cell line NCM460 and human CRC cell lines Lovo, SW48, T84, SW948, LS174T, HT29, HCT116 and SW480 were purchased from Procell Life Sciences Co. Ltd., (Wuhan, Hubei, China). Cell lines NCM460 was cultured in RPMI-1640 (Gibco) medium, T84 in DMEM/F12 (Gibco) medium, Lovo in F12K (Gibco) medium, LS174T in MEM, HT29 and HCT116 in (Gibco) McCoy's 5A, SW48, SW948 and SW480 in L15 (Gibco) medium.

All media for the human cell lines were supplemented with 10% FBS and 1% penicillin/streptomycin antibiotics. SW48, SW948 and SW480 cell lines were cultured in 100% air at 37 °C. Other cell lines were cultured under 95% air-5% CO_2 at 37 °C. All cell lines were validated by STR DNA finger-printing. Experiments were carried out within 6 months after acquisition of the cell lines. In addition, mycoplasma contamination was ruled out using a PCR-based method.

HT29 and LS174T cells were transfected with miR-20a mimic and negative control (NC) or miR-20a inhibitor and inhibitor NC (inNC) respectively using Lipofectamine 2000 (Invitrogen, USA). After 48 h transfection, these cells were harvested for further experiments. These inhibitors and activator, including C75 (inhibitor of FASN), PKI-402 (inhibitor of PI3K/mTOR), MSAB (inhibitor of Wnt/β-catenin), Mycro 3 (inhibitor of Myc) and ZLN024 (activator of AMPK), were purchased from GLPBIO.

2.9.2. Western blotting

The cells were washed with ice-cold PBS and lysed with RIPA buffer containing protease inhibitors. After mixed with SDS sample buffer, the proteins were heated to 99 °C for 10 min, separated on 10% SDS–polyacrylamide gels, transferred to PVDF membranes, and probed with antibodies against β-catenin (1:1000; CST, USA) and β-actin (1:3000, Proteintech, China) at 4 °C overnight and blots were visualized using gel

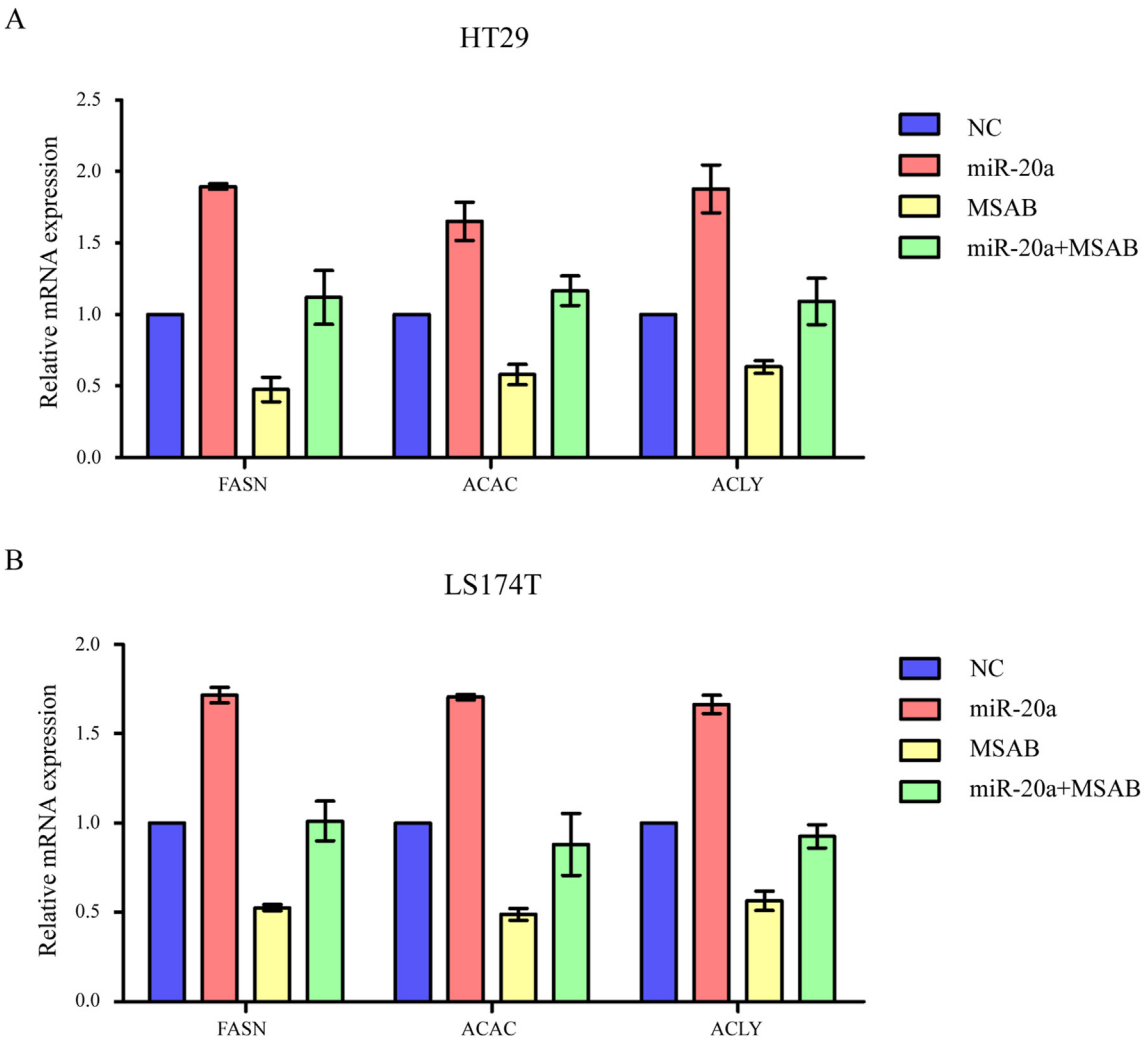

Figure 5. The necessity of the Wnt signaling pathway in miR-20a promoting FA synthesis. (A) HT29 cells. (B) LS174T cells.

imaging systems (Bio-Rad). ECL was used to visualize the immunoblot signals.

2.9.3. Real time-quantitative PCR (RT-qPCR)

Total RNA of HT29 and LS174T cells were extracted using total RNA extraction kit (Thermo Fisher Scientific, Waltham, USA). 1 μg RNA was used for reverse transcription into complementary DNA (cDNA) using the PrimeScript RT-PCR Kit (Takara, Tokyo, Japan). Real-time polymerase chain reaction (RT-PCR) was conducted using the SYBR Premix Ex-Taq II kit (Takara, Tokyo, Japan) on the Quant Studio 3 Real-Time PCR System (Applied Biosystems, CA, USA). The fold changes were determined using the $2^{-\triangle\triangle CT}$ method. All primers used were as follows: Quantitative-FASN, forward 5′-AAGGACCTGTCTAGGTTTGATGC-3′, reverse 5′-TGGCTTCATAGGTGACTTCCA-3’; Quantitative-ACACA, forward 5′-ATGTCTGGCTTGCACCTAGTA-3′ reverse 5′-CCCCAAAGCGAGTAA-CAAATTCT-3’; Quantitative-ACLY, forward 5′-TCGGCCAAGGCAATTT-CAGAG-3′ reverse 5′-CGAGCATACTTGAACCGATTCT-3’; Quantitative-Bactin, forward 5′-CATGTACGTTGCTATCCAGGC-3′ reverse 5′-CTCCTTAATGTCACGCACGAT-3’; Quantitative-U6, forward 5′-CTCGCTTCGGCAGCACATATACT-3′ reverse 5′-ACGCTTCACGAATTT GCGTGTC-3’; Quantitative-miR-20a, forward 5′-TAAAGTGCTTA-TAGTGCAG-3′ reverse 5′-GTCGTATCCAGTGCAGGGTCCGAGGT-3’; Reverse Transcription-miR-20a, 5′-GTCGTATCCAGTGCAGGGTCC-GAGGTATTCGCACTGGATACGACCTACCT-3’; Reverse Transcription-U6, 5′-AAAATATGGAACGCTTCACGAATTTG -3’.

2.9.4. Clone-formation assay, EdU assay, transwell assay and wound-healing assay

For the clone formation assay, HT29 and LS174T cell lines were transfected with mimic/NC (inhibitor/inNC) on day 1. Digest the cells the next day and seed 200 cells into a six-well plate, followed by the addition of 2 ml of 10% FBS DMEM for 14 days. After 14 days, the cells were fixed in 4% paraformaldehyde and stained with crystal violet for 30 min at room temperature. Colonies consisting of >50 cells were counted. For EdU assay, cells were plated in 12-well plates and performed transfection. After 48h, 5-ethynyl-2′-deoxyuridine (EdU) assay (BeyoClick™ EdU-488 Kit, Beyotime, Shanghai, China) were performed to analyze the cell proliferation. The cells were incubated with 10μM EdU solution for 2 h and fixed with 4% paraformaldehyde. And the cells were washed with PBS for 3 times and 0.5% TritonX-100 once. Then, the cells were stained with 100 μL 1 × DAPI solution. After washed with 100μL PBS for 3 times, images were obtained from fluorescence microscope for further calculation of proliferation rates.

Transwell assays were conducted using an 8 μm pore Transwell filter (Corning, US). HT29 or LS174T cells were seeded in the upper chamber with serum-free medium. And medium with 10% FBS was added to the lower chamber. After incubation for 48 h, the Transwell filter was washed, fixed with 4% paraformaldehyde and in turn stained with 0.1% crystal violet staining solution.

For wound-healing assay, HT29 or LS174T cells were seeded on six-well plates. Then, a wound across the wall was introduced. After

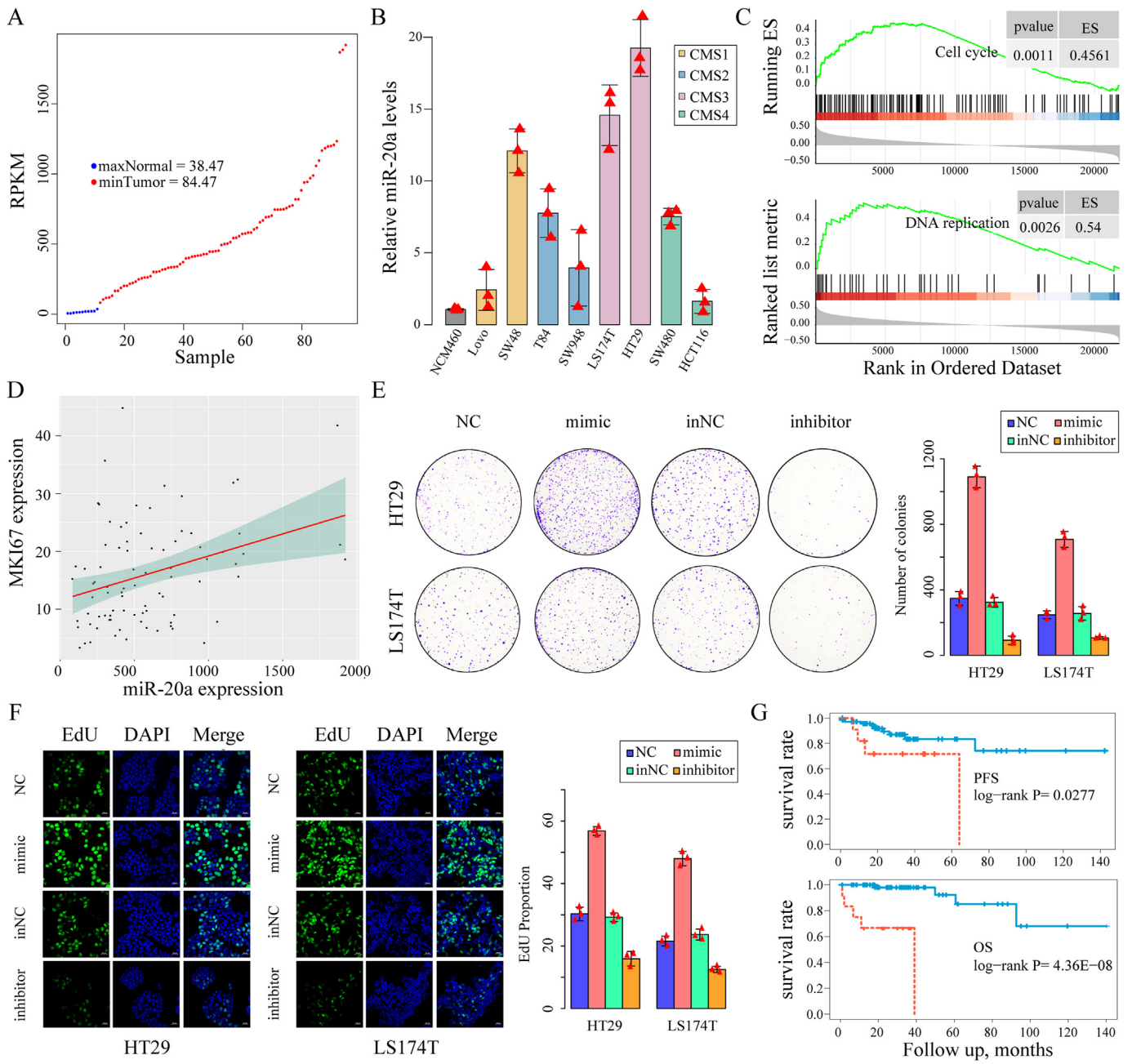

Figure 6. miR-20a affect cell proliferation. (A) The expression of miR-20a across normal colorectal samples (blue) and metabolic CRC samples (red). (B) The expression of miR-20a among CMSs cell lines and one colon epithelial cell line. (A) GSEA showed cell cycle and DNA replicant pathway were upregulated in miR-20a high expression group. (D) Correlation of miR-20a with MKI67 expression. Representative photomicrographs and quantifications of (E) clone formation assay and (F) Edu assay in HT29 and LS174T cells after transfection with miR-20a mimic, miR-20a mimic NC, miR-20a inhibitor, or miR-20a inNC for 14 days. (*$P < 0.05$; **$P < 0.01$; ***$P < 0.001$). (G) K–M curves showed OS and PFS of metabolic CRC patients in miR-20a low and high expression subgroups.

washing with PBS, the plate was incubated with serum-free medium for 24 h. Cell migration was observed and photographed by microscopy.

2.9.5. Immunofluorescence analysis

The cells were seeded on poly-lysine-coated coverslips for 24 h, fixed with 4% paraformaldehyde for 15 min, and permeabilized in 1% Triton X-100 for 10 min. The cells were then blocked with 5% BSA in PBS for 30 min at room temperature and incubated in antibodies overnight at 4 °C. The coverslips were washed three times with PBS buffer, and the secondary antibody was applied for 1 h at 37 °C. The coverslips were then mounted onto glass slides using an antifade mounting medium (Beyotime, China). Cells were then examined under a laser scanning confocal microscope (Zeiss LSM 510 Meta).

2.10. Quantification and statistical analysis

2.10.1. Analysis of RNA-seq data

For RNA-seq data, we used the edgeR algorithm to detect DE genes from raw count data. The Benjamini–Hochberg procedure for multiple testing was used to control the false discovery rate.

2.10.2. Survival analysis

The Kaplan–Meier (K-M) analysis and log-rank test were used to compare survival differences between two groups. We calculated hazard ratios (HRs) and 95% confidence intervals using the univariate Cox proportional hazards model. For illustration purposes, continuous

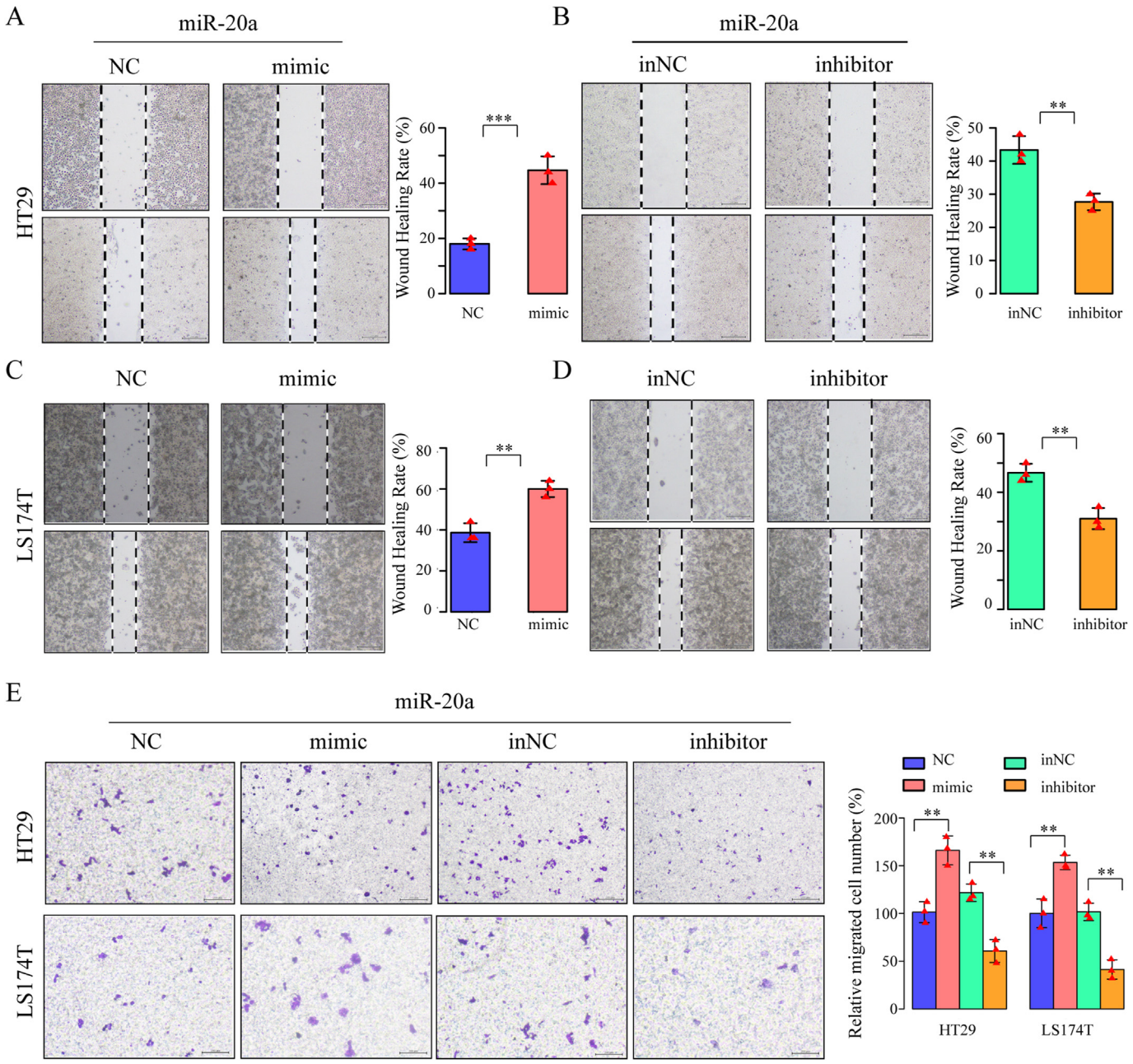

Figure 7. miR-20a promoted migration of metabolic CRC cells. (A–D) Wound healing assay of HT29 and LS174T cells carrying different miRNAs. (E) Transwell assays of HT29 and LS174T cells carrying different miRNAs. Bar = 100μm. Mean ± SD are shown. (*$P < 0.05$; **$P < 0.01$; ***$P < 0.001$).

expression values were dichotomized based on the maximization of the log-rank statistic to generate K-M curves using survminer R package.

2.10.3. Statistical analysis

All statistical analyses were performed using R software version 3.6.3 (http://www.r-project.org/).

3. Results

3.1. Multi-omics data defines functional miRNAs in metabolic subtype

To elucidate regulatory mechanisms underlying the metabolic CRC, we inferred a microRNA regulatory network to identify functional miRNAs (Fmirs) linked to activated metabolism by initially defining Mgenes. Firstly, we summarized metabolism-related genes that were significantly frequently up- or down-regulated in metabolic CRC from the individual-level genes identified by RankComp algorithm (Cumulative binomial model, adjusted $P < 0.05$). Mgenes were defined as the top-ranked 100 metabolism-related genes with highest aggregated multi-omics scores from genome, epigenome, transcriptome and interactome (Table S2). For metabolic CRC cell line HT29, Mgenes showed significantly lower dependency scores than other genes using RNAi data (Figure 1A), indicating their critical roles for cancer cell growth. Besides, Mgenes were significantly enriched with tumor driver genes identified by TUSON explorer (Davoli et al., 2013) (Figure 1B), and can separate metabolic CRC from normal samples (Figure 1C). Moreover, each Mgene was significantly correlated with at least one metabolite abundance using CCLE-CRC data (Median = 11 and mean = 13.47; Pearson correlation analysis, $P < 0.05$; Figure 1D), indicating Mgenes are likely to alter cellular metabolism.

We inferred that the miRNAs whose targets were enriched with Mgenes were essential for activated metabolism in metabolic CRC. Then,

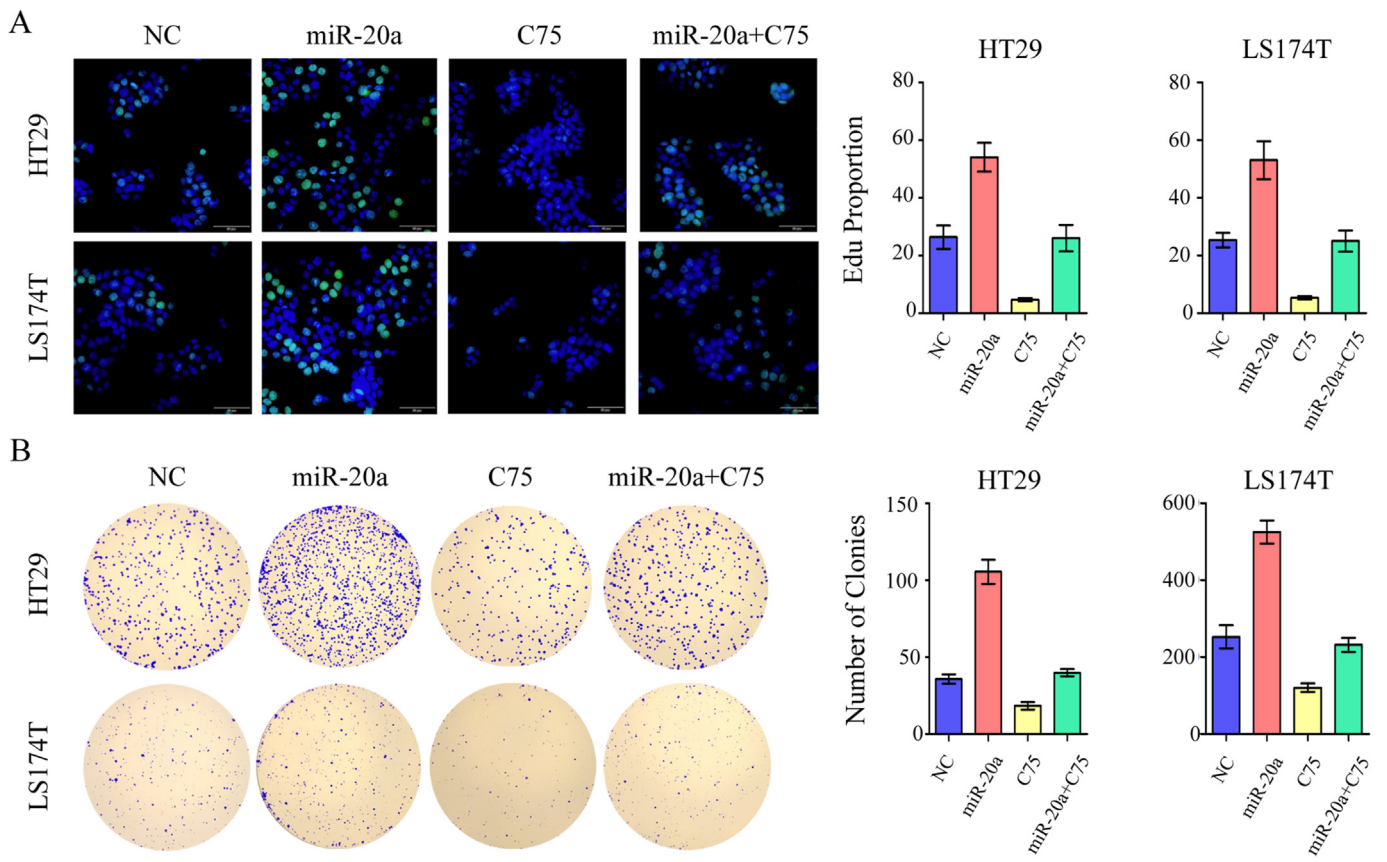

Figure 8. Evaluating the effect of FA synthesis on miR-20a expression promoting cell proliferation. (A) Edu assay. (B) Clone-formation assay.

we identified significantly correlated miRNA-gene interactions in metabolic CRC using paired miRNA and mRNA expression data from TCGA (Pearson correlation analysis, $P < 0.05$ and $|\rho|>0.3$). Taking the significant interacting genes as a gene set signature for each miRNA, we applied sigQC version 0.1.20, an R package to evaluate the basic statistical properties of gene set signatures underlying their applicability across datasets. We ran this package on all combinations of 12 datasets and 100 signatures, and found that CRC datasets are comparable in quality for the application of the gene set signature (Figure 1E; taken miR-20a as an example).

Thus, we inferred a miRNA regulatory network by integrative analysis of Mgenes expression and miRNA expression profiles in the TCGA dataset to identify miRNAs linked to activated metabolism in metabolic CRC (Figure S1). The target genes of 12 miRNAs were enriched with Mgenes and these miRNAs were defined as Fmirs linked to activated metabolism (Eq. (1): Hypergeometric test, $P < 0.05$), 11 of which were significantly deregulated in metabolic CRC compared to normal samples. Besides, targets of several Fmirs such as miR-363, miR-20a and miR-148a, were significantly overrepresented at the top of gene list in ascending order in the RNAi and CRISPR screened metabolic CRC cell line HT29 (GSEA, $P < 0.05$; Figure 1F), indicating their critical roles for cancer cell growth. These Fmirs were also significantly enriched with driver miRNA of CRC collected from miRCancer and OncomiRDB databases (Hypergeometric test, $P < 0.05$; red in Figure 1G). Hierarchical clustering analysis found that the 12 Fmirs can separate metabolic CRC samples from normal samples (Figure 1G). Seven of the 12 Fmirs were measured by CCLE-CRC miRNA expression profiles. Compared with metabolite abundance profiles of CRC in CCLE, triacylglycerol (TAG) which is the storage form of fatty acid, correlated more Fmirs than non-TAG (Student's T-test, $P = 7.45E-04$; Figure 1H) and each Fmir was significantly correlated with at least nine metabolite abundances (Pearson correlation analysis, $P < 0.05$; Figure 1I). Among these Fmirs, miR-20a correlated with the most metabolites.

3.2. *miR-20a promoted FA synthesis metabolism in metabolic CRC*

We also observed an interesting positive association of miR-20a with TAG (Figure 2A). Metabolic CRC is characterized by prominent metabolic activation, exhibiting significantly higher enrichment score (ES) in FA metabolism pathway than the other subtypes (Figure 2B). Accumulating evidence suggests that alterations in lipid metabolism represented by FA metabolism, contribute to overall metabolic reprogramming in cancer cells (Carracedo et al., 2013; Currie et al., 2013). To identify putative master regulators for the aberrant metabolism in metabolic CRC, we identified FA metabolism subpathway mediated by Fmirs. The subpathway contained 34 consecutive differential molecules, including miR-20a (Figure 2C). GSEA revealed that miR-20a was enriched in hallmark gene set of FA metabolism by integrative analysis of gene expression and miRNA expression profiles in the TCGA (Figure 2D). What's more, the expression of miR-20a was significantly correlated with the protein expression of FA synthesis enzymes *FASN* and *ACAC* (Figure 2E-F). Thus, miR-20a may be essential for FA metabolism in metabolic CRC.

The HT29 and LS174T cells were transfected with miR-20a mimic, miR-20a inhibitor or NC to analyze multiple FA synthesis related genes, including *FASN*, *ACAC* and *ACLY*. We observed that transfected miR-20a mimic into HT29 and LS174T cell lines up-regulated the expression of miR-20a (Figure 2G). Simultaneously, the expression of *FASN*, *ACAC* and *ACLY* were increased in response to miR-20a mimic versus NC (Figure 2H). The subsequent loss-of-function experiments revealed that HT29 and LS174T cells transfected with miR-20a inhibitor had diminished miR-20a, *FASN*, *ACAC* and *ACLY* expressions compared with inNC

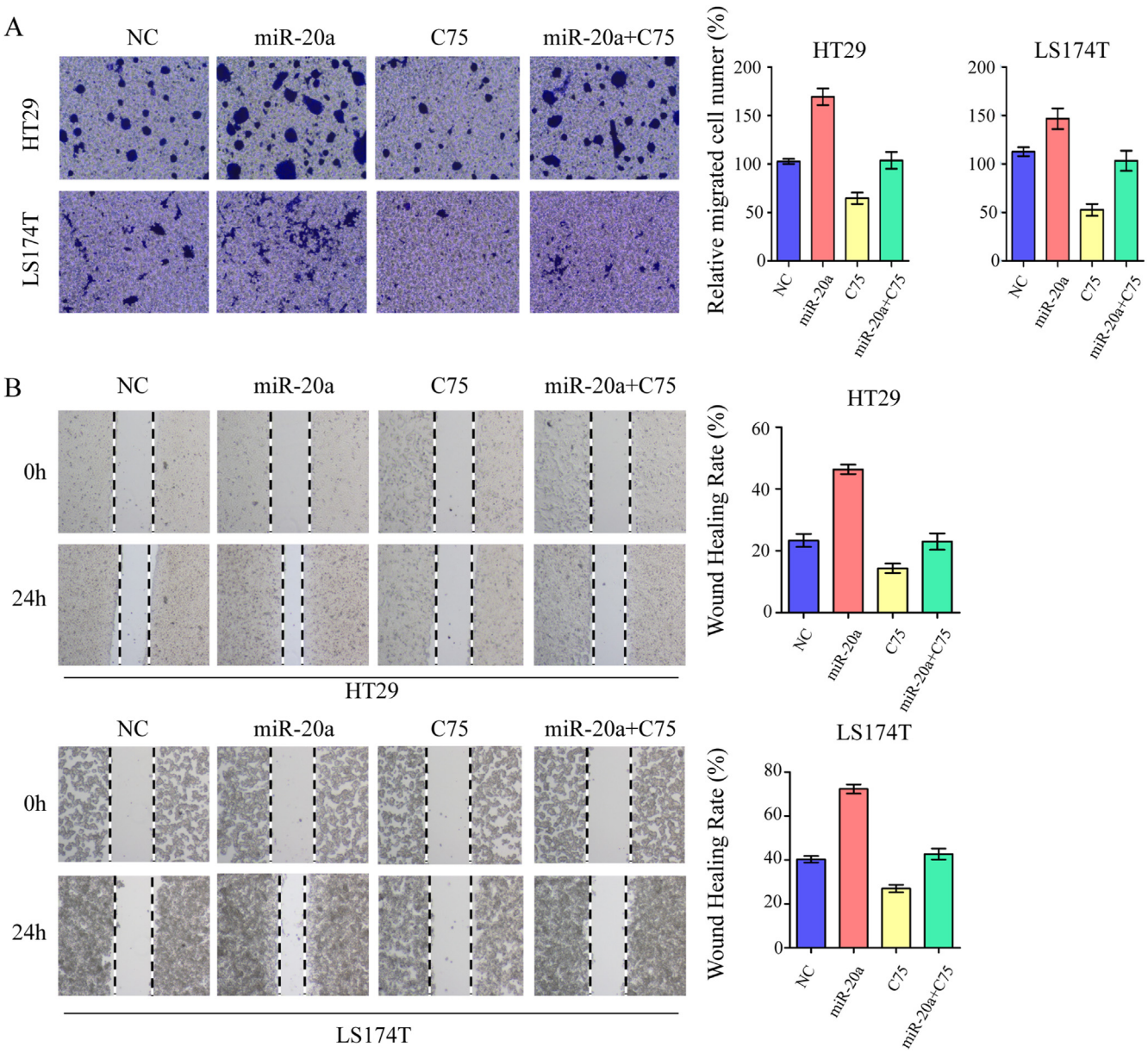

Figure 9. Evaluating the effect of FA synthesis on miR-20a expression promoting cell migration. (A) Transwell assay. (B) Wound healing assay.

groups (Figure 2I-J). These results indicated that up-regulation of miR-20a promoted FA synthesis in metabolic CRC.

3.3. *miR-20a promotes FA synthesis via Wnt signaling pathway*

To identify the key pathways by which miR-20a promotes FA synthesis, we screened potential FA synthesis related pathways using inhibitors/activators, including PI3K/AKT/mTOR, Wnt, Myc and AMPK pathway. We co-treated HT29 and LS174T with miR-20a and these inhibitors/activators and found that the effect of miR-20a on FA synthesis was rescued only after inhibiting Wnt signaling pathway (Figure 3). The target Mgene *FOXQ1* of miR-20a, which can regulate liver metabolism (Cui et al., 2016), is a marker for activation of Wnt signaling in solid tumors (Christensen et al., 2013). Activation of the Wnt signaling pathway led to lipid accumulation in cells (Terrand et al., 2009). Thus, we inferred that miR-20a promoted FA synthesis via Wnt signaling pathway in metabolic CRC. Using ssGSEA, we calculated the enrichment score of Wnt gene sets listed in MSigDB. The expression of miR-20a was significantly positively correlated with canonical Wnt signaling pathway (Pearson correlation analysis, $P = 0.0108$, $\rho = 0.2766$), but negatively correlated with non-canonical Wnt signaling pathway (Pearson correlation analysis, $P = 0.0176$, $\rho = -0.2585$). The canonical Wnt signaling pathway causes an accumulation of β-catenin in the cytoplasm and induce a cellular response. Therefore, we sought to determine whether Wnt participated in miR-20a induced FA synthesis through exploring the effects on β-catenin expression.

After transfecting miR-20a mimic, inhibitor, and paired NC, the expression of β-catenin was detected by western blotting (WB) and immunofluorescence (IF) in HT29 and LS174T cell lines. As expected, WB analysis showed that miR-20a mimic-treated cells expressed higher β-catenin compared with NC groups (Figure 4A), whereas lower β-catenin was detected in miR-20a inhibitor-treated cells (Figure 4B). miR-20a mimic-treated HT29 cells also showed significantly higher β-catenin positive staining counts than the NC group (Figure 4C). In contrast, miR-20a inhibitor-treated HT29 cells showed a reversed phenotype. We obtained similar results in LS174T cell line (Figure S2). The results suggest that miR-20a promotes Wnt/β-catenin level in metabolic CRC cell lines. Previous studies have reported that the activated Wnt signaling

pathway can up-regulate the activity of FA synthesis in tumor. Therefore, we used LiCl (10 mmol/L) to treat HT29 and LS174T cells to activate Wnt signaling pathway and analyze the expression of FA-related genes. The results showed that activating the Wnt signaling pathway can significantly promote the up-regulation of FA metabolism genes (*FASN*, *ACAC* and *ACLY*) in metabolic CRC cell lines (Figure 4D).

Then, we performed a rescue experiment to test the necessity of the Wnt signaling pathway in miR-20a promoting FA synthesis. In short, we treated the HT29 and LS174T with Wnt inhibitor (MSAB) after overexpressing the level of miR-20. Next, we analyzed the expression of FA metabolic genes. After inhibiting the Wnt signaling pathway, miR-20a could not upregulate the expression of FA metabolism genes. And we found that the Wnt signaling pathway is essential for miR-20a to promote the expression of FA synthesis related genes (Figure 5).

3.4. Elevated miR-20a promoted proliferation and migration of metabolic CRC

Importantly, miR-20a is minimally expressed in normal colorectal tissues, suggesting the potential of targeting miR-20a for therapeutic purposes (Figure 6A). Compared with colon epithelial cell line NCM460 and other non-metabolic CRC cell lines, we further observed significantly up-regulated expressions of miR-20a in metabolic CRC cell lines HT29 and LS174T by RT-qPCR assays (Figure 6B). GSEA was run to explore the potential role of miR-20a in CMS3 and showed that miR-20a played an important role in promoting cell cycle and DNA replicant (adjusted $P < 0.05$; Figure 6C). Besides, expression of miR-20a was significantly correlated with the proliferation marker *MKI67* (Pearson correlation analysis, $P = 1.72E\text{-}03$, $\rho = 0.34$; Figure 6D). Then, we took on experiments to investigate miR-20a function during CRC tumorigenesis. The effects of miR-20a on cell proliferation of HT29 and LS174T cells were examined using clone-formation assay. The assay showed that elevated miR-20a expression promoted the clone formation ability of HT29 cells compared with NC groups. In contrast, miR-20a inhibitor-treated HT29 cells showed a reversed phenotype. We repeated these experiments in LS174T cells and received coherent outcomes (Figure 6E). EdU assay showed that miR-20a promoted proliferation of HT29 and LS174T cells compared to NC groups (Figure 4F). While inhibition of miR-20a will reduce cell proliferation, suggesting that miR-20a had a critical role in metabolic CRC tumor proliferation.

We performed wound healing assay and transwell assay to determine the effect of miR-20a on the migration ability of metabolic CRC cell lines. In the wound healing assay, cell motility was monitored at designated time points after scratches. The miR-20a overexpressed cells migrated toward the wound more quickly than the NC groups (Figure 7A). In contrast, miR-20a inhibitor-treated HT29 cells showed a reversed phenotype (Figure 7B). We repeated these experiments in LS174T cells and received coherent outcomes, suggesting that miR-20a had a unanimous pivotal role in metabolic CRC oncogenesis, that is, inducing tumor migration in vitro (Figure 7C-D). A cell migration assay in a transwell system was performed to further assess the effect of miR-20a on HT29 cell migration. Our results showed that transfection with miR-20a mimic in HT29 cells effectively increased the migratory abilities (Figure 7E). In contrast, the migratory abilities exerted reversed trend in miR-20a inhibitor-treated HT29 cells. Moreover, miR-20a expression is prognostic of both overall survival (OS) and progression-free survival (PFS) of metabolic CRC in TCGA data (Figure 6G).

3.5. FA synthesis is essential for miR-20a to promote CMS3-CRC proliferation and migration

We have test that miR-20a promotes FA metabolism via Wnt signaling pathway in metabolic CRC cell lines. Then, we performed rescue experiments to prove the contribution of FA synthesis in miR-20a promoting CMS3-CRC proliferation and migration. Briefly, we overexpressed miR-20a and treated with FASN inhibitor (C75) in HT29 and LS174T cells, respectively. Next, we performed Edu assay (Figure 8A) and clone-formation assay (Figure 8B). The assays showed that elevated miR-20a expression promoted cell proliferation, and blocking FA synthesis by C75 can inhibited this effect. In addition, we performed transwell assay (Figure 9A) and wound healing assay (Figure 9B) to observe cell migration ability. Intriguingly, inhibiting FA synthesis can impair the wound-healing ability and cell migration of CMS-CRC cells, and partially rescue the effect of miR-20a to promote cell migration. These results suggest that miR-20a promotes CMS3-CRC cell migration and proliferation through FA synthesis.

4. Discussion

In recent years, the CMSs, which are emerging as critical factor for prognosis and treatment of CRC, have attracted wide attention. We have identified a core set of functional gene regulators for each CMS by integrating multi-omics data. FGRs played critical roles in regulating immune microenvironment of CMSs. miRNAs are also gene regulators serving an important role in tumorigenic processes. Thus, we identified 12 Fmirs associated with metabolic CRC based on Mgenes integrating from multi-omics features. Fmirs played a critical role in metabolic CRC cell growth and FA metabolism pathway.

Consistent with our finding, the Fmir miR-20a has been documented to be highly expressed in CRC tissues versus normal mucosal tissues (Xu et al., 2015), and this up-regulation in CRC has also been confirmed in serum and plasma (Yau et al., 2016). Beyond these findings, we demonstrated that miR-20a promoted FA synthesis in metabolic CRC. Activation of the Wnt signaling pathway led to lipid accumulation in cells (Terrand et al., 2009). We further found that miR-20a up-regulated Wnt/β-catenin signaling by systematically coupling bioinformatics analyses and in vitro experiments. β-catenin is a major component of cell-cell adhesion structures and functions as a controller of cell migration, colony formation and stem cell properties through translocation into nucleus (Dobrosotskaya and James, 2000; Wang et al., 2017). Aberrant β-catenin accumulation in the cytoplasm usually translocates to the nucleus and was associated with tumor relapse and metastasis in breast cancer patients (Bui et al., 2017). The underlying mechanism needs to be further explored. Finally, we found that proliferation and migration abilities of the miR-20a overexpressed cells were significantly promoted, whereas the proliferation and migration abilities were lower in the miR-20a inhibitor groups. Inhibition of miR-20a serve as a potential therapy for metabolic CRC, which need to be further explored.

In conclusion, miR-20a could promote the proliferative and migration in metabolic CRC via regulating fatty acid metabolism and Wnt signaling pathway, highlighting novel mechanisms associated with metabolic CRC cancerogenesis.

5. Limitations of study

Our study has distinct limitations. We revealed miR-20a as the most powerful determinant that regulates a cascade of dysregulated events in metabolic CRC, including Wnt signaling pathway and core enzymes involved in FA metabolism program by bioinformatics analyses and in vitro assays. We also showed the relevance of miR-20a with triacylglycerol abundances. However, we did not directly test the regulation of miR-20a in the metabolite abundances of FA metabolism. These experiments should be done in the future. The tumor microenvironment, which lacks in cell lines models, plays a significant role in cancer. Future in vivo assays should assess miR-20a function in metabolic CRC.

Declarations

Author contribution statement

Kai Song: Conceived and designed the experiments; Analyzed and interpreted the data; Wrote the paper.

Chao Liu: Conceived and designed the experiments; Performed the experiments; Wrote the paper.

Jiashuai Zhang; Huiting Xiao: Analyzed and interpreted the data.

Yang Yao: Performed the experiments.

Rongqiang Yuan; Keru Li; Jia Yang: Contributed reagents, materials, analysis tools or data.

Wenyuan Zhao; Yanqiao Zhang: Conceived and designed the experiments; Wrote the paper.

Funding statement

This study was supported by Guangdong Basic and Applied Basic Research Foundation (2021A1515110238); the National Natural Science Foundation of China (81572935 and 81872427); the Applied Technology Research and Development Program of Heilongjiang Province (GA19C002).

Data availability statement

Data included in article/supplementary material/referenced in article.

Declaration of interests statement

The authors declare no conflict of interest.

Additional information

Supplementary content related to this article has been published online at https://doi.org/10.1016/j.heliyon.2022.e09068.

References

Bartel, D.P., 2018. Metazoan MicroRNAs. Cell 173, 20–51.
Bruning, U., Morales-Rodriguez, F., Kalucka, J., Goveia, J., Taverna, F., Queiroz, K.C.S., Dubois, C., Cantelmo, A.R., Chen, R., Loroch, S., et al., 2018. Impairment of angiogenesis by fatty acid synthase inhibition involves mTOR malonylation. Cell Metabol. 28, 866–880 e815.
Bui, T., Schade, B., Cardiff, R.D., Aina, O.H., Sanguin-Gendreau, V., Muller, W.J., 2017. beta-Catenin haploinsufficiency promotes mammary tumorigenesis in an ErbB2-positive basal breast cancer model. Proc. Natl. Acad. Sci. U. S. A. 114, E707–E716.
Carracedo, A., Cantley, L.C., Pandolfi, P.P., 2013. Cancer metabolism: fatty acid oxidation in the limelight. Nat. Rev. Cancer 13, 227–232.
Chan, B., Manley, J., Lee, J., Singh, S.R., 2015. The emerging roles of microRNAs in cancer metabolism. Cancer Lett. 356, 301–308.
Christensen, J., Bentz, S., Sengstag, T., Shastri, V.P., Anderle, P., 2013. FOXQ1, a novel target of the Wnt pathway and a new marker for activation of Wnt signaling in solid tumors. PLoS One 8, e60051.
Cui, Y., Qiao, A., Jiao, T., Zhang, H., Xue, Y., Zou, Y., Cui, A., Fang, F., Chang, Y., 2016. The hepatic FOXQ1 transcription factor regulates glucose metabolism in mice. Diabetologia 59, 2229–2239.
Currie, E., Schulze, A., Zechner, R., Walther, T.C., Farese Jr., R.V., 2013. Cellular fatty acid metabolism and cancer. Cell Metabol. 18, 153–161.
Davoli, T., Xu, A.W., Mengwasser, K.E., Sack, L.M., Yoon, J.C., Park, P.J., Elledge, S.J., 2013. Cumulative haploinsufficiency and triplosensitivity drive aneuploidy patterns and shape the cancer genome. Cell 155, 948–962.
Dhawan, A., Barberis, A., Cheng, W.C., Domingo, E., West, C., Maughan, T., Scott, J.G., Harris, A.L., Buffa, F.M., 2019. Guidelines for using sigQC for systematic evaluation of gene signatures. Nat. Protoc. 14, 1377–1400.
Dobrosotskaya, I.Y., James, G.L., 2000. MAGI-1 interacts with beta-catenin and is associated with cell-cell adhesion structures. Biochem. Biophys. Res. Commun. 270, 903–909.
Eide, P.W., Bruun, J., Lothe, R.A., Sveen, A., 2017. CMScaller: an R package for consensus molecular subtyping of colorectal cancer pre-clinical models. Sci. Rep. 7, 16618.
Feng, L., Xu, Y., Zhang, Y., Sun, Z., Han, J., Zhang, C., Yang, H., Shang, D., Su, F., Shi, X., et al., 2015. Subpathway-GMir: identifying miRNA-mediated metabolic subpathways by integrating condition-specific genes, microRNAs, and pathway topologies. Oncotarget 6, 39151–39164.
Guinney, J., Dienstmann, R., Wang, X., de Reynies, A., Schlicker, A., Soneson, C., Marisa, L., Roepman, P., Nyamundanda, G., Angelino, P., et al., 2015. The consensus molecular subtypes of colorectal cancer. Nat. Med. 21, 1350–1356.
Hammond, S.M., 2015. An overview of microRNAs. Adv. Drug Deliv. Rev. 87, 3–14.
Huang, H.Y., Lin, Y.C., Li, J., Huang, K.Y., Shrestha, S., Hong, H.C., Tang, Y., Chen, Y.G., Jin, C.N., Yu, Y., et al., 2020. miRTarBase 2020: updates to the experimentally validated microRNA-target interaction database. Nucleic Acids Res. 48, D148–D154.
Jones, S.F., Infante, J.R., 2015. Molecular pathways: fatty acid synthase. Clin. Cancer Res. 21, 5434–5438.
Karagkouni, D., Paraskevopoulou, M.D., Chatzopoulos, S., Vlachos, I.S., Tastsoglou, S., Kanellos, I., Papadimitriou, D., Kavakiotis, I., Maniou, S., Skoufos, G., et al., 2018. DIANA-TarBase v8: a decade-long collection of experimentally supported miRNA-gene interactions. Nucleic Acids Res. 46, D239–D245.
Kim, J., DeBerardinis, R.J., 2019. Mechanisms and implications of metabolic heterogeneity in cancer. Cell Metabol. 30, 434–446.
Kim, V.N., Han, J., Siomi, M.C., 2009. Biogenesis of small RNAs in animals. Nat. Rev. Mol. Cell Biol. 10, 126–139.
Kolde, R., Laur, S., Adler, P., Vilo, J., 2012. Robust rank aggregation for gene list integration and meta-analysis. Bioinformatics 28, 573–580.
Li, X., Chen, Y.T., Josson, S., Mukhopadhyay, N.K., Kim, J., Freeman, M.R., Huang, W.C., 2013. MicroRNA-185 and 342 inhibit tumorigenicity and induce apoptosis through blockade of the SREBP metabolic pathway in prostate cancer cells. PLoS One 8, e70987.
Long, J., Zhang, C.J., Zhu, N., Du, K., Yin, Y.F., Tan, X., Liao, D.F., Qin, L., 2018. Lipid metabolism and carcinogenesis, cancer development. Am. J. Cancer Res. 8, 778–791.
Moody, L., Dvoretskiy, S., An, R., Mantha, S., Pan, Y.X., 2019. The efficacy of miR-20a as a diagnostic and prognostic biomarker for colorectal cancer: a systematic review and meta-analysis. Cancers 11.
Paczkowska, M., Barenboim, J., Sintupisut, N., Fox, N.S., Zhu, H., Abd-Rabbo, D., Mee, M.W., Boutros, P.C., Drivers, P., Functional Interpretation Working G, et al., 2020. Integrative pathway enrichment analysis of multivariate omics data. Nat. Commun. 11, 735.
Song, K., Cai, H., Zheng, H., Yang, J., Jin, L., Xiao, H., Zhang, J., Zhao, Z., Li, X., Zhao, W., Li, X., 2021. Multilevel prioritization of gene regulators associated with consensus molecular subtypes of colorectal cancer. Briefings Bioinf.
Song, K., Lu, H., Jin, L., Wang, K., Guo, W., Zheng, H., Li, K., He, C., You, T., Fu, Y., et al., 2020. Qualitative Ras pathway signature for cetuximab therapy reveals resistant mechanism in colorectal cancer. FEBS J. 287, 5236–5248.
Sottoriva, A., Kang, H., Ma, Z., Graham, T.A., Salomon, M.P., Zhao, J., Marjoram, P., Siegmund, K., Press, M.F., Shibata, D., Curtis, C., 2015. A Big Bang model of human colorectal tumor growth. Nat. Genet. 47, 209–216.
Szklarczyk, D., Gable, A.L., Lyon, D., Junge, A., Wyder, S., Huerta-Cepas, J., Simonovic, M., Doncheva, N.T., Morris, J.H., Bork, P., et al., 2019. STRING v11: protein-protein association networks with increased coverage, supporting functional discovery in genome-wide experimental datasets. Nucleic Acids Res. 47, D607–D613.
Terrand, J., Bruban, V., Zhou, L., Gong, W., El Asmar, Z., May, P., Zurhove, K., Haffner, P., Philippe, C., Woldt, E., et al., 2009. LRP1 controls intracellular cholesterol storage and fatty acid synthesis through modulation of Wnt signaling. J. Biol. Chem. 284, 381–388.
Wang, C., Ruan, P., Zhao, Y., Li, X., Wang, J., Wu, X., Liu, T., Wang, S., Hou, J., Li, W., et al., 2017. Spermidine/spermine N1-acetyltransferase regulates cell growth and metastasis via AKT/beta-catenin signaling pathways in hepatocellular and colorectal carcinoma cells. Oncotarget 8, 1092–1109.
Wang, D., Gu, J., Wang, T., Ding, Z., 2014. OncomiRDB: a database for the experimentally verified oncogenic and tumor-suppressive microRNAs. Bioinformatics 30, 2237–2238.
Wang, H., Sun, Q., Zhao, W., Qi, L., Gu, Y., Li, P., Zhang, M., Li, Y., Liu, S.L., Guo, Z., 2015. Individual-level analysis of differential expression of genes and pathways for personalized medicine. Bioinformatics 31, 62–68.
Xiao, F., Zuo, Z., Cai, G., Kang, S., Gao, X., Li, T., 2009. miRecords: an integrated resource for microRNA-target interactions. Nucleic Acids Res. 37, D105–110.
Xiao, Z., Chen, S., Feng, S., Li, Y., Zou, J., Ling, H., Zeng, Y., Zeng, X., 2020. Function and mechanisms of microRNA-20a in colorectal cancer. Exp. Ther. Med. 19, 1605–1616.
Xie, B., Ding, Q., Han, H., Wu, D., 2013. miRCancer: a microRNA-cancer association database constructed by text mining on literature. Bioinformatics 29, 638–644.
Xu, T., Jing, C., Shi, Y., Miao, R., Peng, L., Kong, S., Ma, Y., Li, L., 2015. microRNA-20a enhances the epithelial-to-mesenchymal transition of colorectal cancer cells by modulating matrix metalloproteinases. Exp. Ther. Med. 10, 683–688.
Yau, T.O., Wu, C.W., Tang, C.M., Chen, Y., Fang, J., Dong, Y., Liang, Q., Ng, S.S., Chan, F.K., Sung, J.J., Yu, J., 2016. MicroRNA-20a in human faeces as a non-invasive biomarker for colorectal cancer. Oncotarget 7, 1559–1568.
Zhang, H., Niu, Q., Liang, K., Li, X., Jiang, J., Bian, C., 2021. Effect of LncPVT1/miR-20a-5p on lipid metabolism and insulin resistance in NAFLD. Diab. Metabol. Syndr. Obes. 14, 4599–4608.
Zhou, K.R., Liu, S., Sun, W.J., Zheng, L.L., Zhou, H., Yang, J.H., Qu, L.H., 2017. ChIPBase v2.0: decoding transcriptional regulatory networks of non-coding RNAs and protein-coding genes from ChIP-seq data. Nucleic Acids Res. 45, D43–D50.